Synthesis and Morphology of Molecular Brushes with Polyacrylonitrile Block Copolymer Side Chains and Their Conversion into Nanostructured Carbons

Chuanbing Tang,† Bruno Dufour, Tomasz Kowalewski,* and Krzysztof Matyjaszewski*

Department of Chemistry, Carnegie Mellon University, 4400 Fifth Avenue, Pittsburgh, Pennsylvania 15213

Received April 16, 2007; Revised Manuscript Received June 14, 2007

ABSTRACT: Densely grafted brushes with polyacrylonitrile (PAN) di- (AB) and triblock (ABC) copolymer side chains were synthesized first time by ATRP using the "grafting from" technique. Tapping-mode atomic force microscopy showed that these brushes displayed wormlike shapes on mica surface. A necklacelike structure was observed for brushes with poly(*n*-butyl acrylate)-*b*-polyacrylonitrile-*b*-poly(*tert*-butyl acrylate) triblock copolymer side chains. After conversion of poly(*tert*-butyl acrylate) side chains to poly(acrylic acid), they were cross-linked with diamine to fix the extended 3-dimensional structure. Such shell-cross-linked molecular brushes showed improved stability during transferring from solution to flat substrates and have been successfully converted into nanostructured carbons through pyrolysis. The pyrolyzed materials exhibited characteristics of partially graphitic carbon.

Introduction

Densely grafted molecular brushes have been attracting considerable attention from theoreticians and experimentalists due to their well-defined hierarchical molecular architecture and their potential use as sensors and components of advanced materials.[1−14] Traditionally, molecular brushes are prepared by "grafting through" procedures which involve the synthesis of well-controlled macromonomers by living ionic polymerization, under stringent process conditions, followed by conventional free radical polymerization of the macromonomers.[2,15] This approach provides products with poor overall control over the final topology of the macromolecule. In the past decade, controlled/living radical polymerizations, particularly atom transfer radical polymerization (ATRP),[16−21] have opened a convenient route, (mainly using the "grafting from" strategy), to the preparation of well-defined molecular brushes. The "grafting from" approach employs a backbone with functional side groups that allow the formation of uniform side chains bearing high chain end functionality, which can be used for further chain-extension reactions in order to incorporate property-targeted segments.[7,22−26] To date, both polyacrylates and polymethacrylates have been utilized as the backbone. As side chains, poly(*n*-butyl acrylate) PBA,[22,23,26−28] poly(*tert*-butyl acrylate) (PtBA),[7] polystyrene (PS),[7] poly(*N*-isopropyl acrylamide) (PNIPAM)[29] and poly(2-(dimethylamino)ethyl methacrylate (PDMAEMA)[30−32] were successfully grafted from backbones. Molecular brushes with diblock copolymers as side chains have also been prepared, including PBA-*b*-PS and PS-*b*-PBA,[33] PS-*b*-P*t*BA, P*t*BA-*b*-PS, PS-*b*-poly(acrylic acid) (PAA) and PAA-*b*-PS,[7] PBA-*b*-polycaprolactone[34] and poly(*tert*-butyl methacrylate)-*b*-poly(methyl methacrylate) (PBMA-*b*-PMMA).[35]

Because of the large intrinsic size (tens of nanometers),[36] single brush macromolecules can be relatively easily visualized with AFM. It has been established by AFM that PBA, poly(ethylene oxide) (PEO)[24]and PNIPAM side chains can spread out on a mica surface forming structures, in which the individual graft chains can be visualized with molecular resolution. These conformations are dynamic, since brushes with PBA side chains can undergo a conformational transition from wormlike to globular shapes, depending on the presence of solvent in the environment.[37−40] This transformation resembles one observed upon the change of the lateral pressure in brush monolayers spread on a liquid subphase.[26] More recent [15]reports indicate also that adsorption of brushlike macromolecules with long side chains on a substrate can induce not only conformational deformations but also spontaneous rupture of covalent bonds in the macromolecular backbone.[41] Brushes with hydrophobic PS and PtBA side chains either exhibit a globular conformation or form aggregates due to poor interaction with mica or silicon wafer substrates. Meanwhile, molecular brushes with diblock copolymers as side chains were visualized by AFM as wormlike structures, but without molecular resolution of the side chains,[7,33,35] indicating that side chains on the surface adopt a collapsed rather than extended conformation.

Work described herein had several important elements of novelty. To date, there have been no reports on the synthesis of brushes with ABC triblock copolymer side chains. It is well-known that the phase diagram of ABC triblock copolymers is much more complicated than that of simple AB diblocks.[42] The third block of side chains may additionally influence the solution conformation of brushes through microphase separation effects, and may affect the behavior of side chains when the brushes are deposited on the surface. Brushes with block copolymer containing PAN segments in the side chains have not been yet prepared. Moreover, to the best of these authors' knowledge, the attempt presented here to convert brushes into shape-persistent nanoobjects by shell cross-linking[43] has only one precedent in literature reported by Wooley et al.[44]

One of our motivations for incorporation of PAN is to prepare discrete carbon nanostructures.[45−48] Thus, we designed molecular brush with a layer of PAN around the backbone. This layer can be then converted into carbon while the backbone and the

* Corrrsponding authors. E-mail: (T.K.) tomek@andrew.cmu.edu; (K.M.) km3b@andrew.cmu.edu.

† Current address: Materials Research Laboratory, University of California, Santa Barbara, California 93106.

10.1021/ma070892o CCC: $37.00
Published on Web 07/31/2007

Scheme 1. Shell Cross-Linked Molecular Brushes and Their Conversion into Nanostructured Carbons Through Thermal Treatment

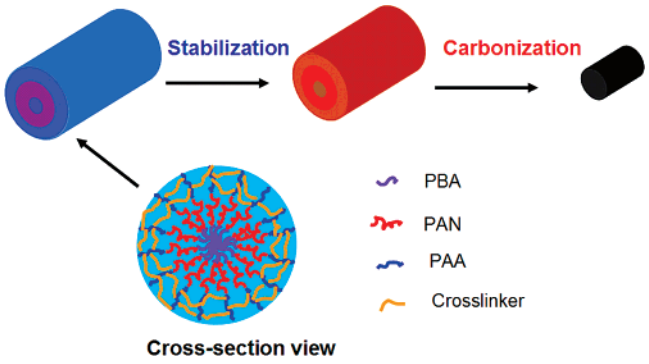

inner layer and the outer cross-linked layer can be removed through pyrolysis.

Well-defined brushes with polymethacrylate backbone and side chains comprised of PBA-*b*-PAN or PBA-*b*-PAN-*b*-PtBA block were synthesized by ATRP. As shown in Scheme 1, PAN serving as carbon precursor was placed as a middle block of side chains sandwiched between the outer shell and the inner core made up of sacrificial blocks.

Experimental Section

Materials. *n*-Butyl acrylate (BA), *tert*-butyl acrylate (tBA), acrylonitrile (AN) and 2-(trimethylsilyloxy)ethyl methacrylate (HEMA-TMS) were purchased from Aldrich and distilled under vacuum. Cu(I)Br and Cu(I)Cl were obtained from Aldrich and purified according to published procedures.[49] 4,4′-Di(5-nonyl)-2,2′-bipyridine (dNbpy) was prepared as described elsewhere.[50] *N*,*N*,*N*′,*N*″,*N*″-pentamethyldiethylenetriamine (PMDETA), trifluoroacetic acid (TFA), dimethylformamide (DMF), $CuCl_2$, and 2,2′-bipyridine (bpy), 2,2′-(ethylenedioxy)bis(ethylamine), carbodiimide (1-[3′-(dimethylamino)propyl]-3-ethylcarbodiimide methiodide), dicyclohexyl, dimethylaminopyridine, anisole, and methanol were used as received from Aldrich.

Typical Polymerization Procedures. Poly(HEMA-TMS) and poly(2-(2-bromopropionyloxy)ethyl methacrylate) (PBPEM) (**B0**, $M_n = 76\,000$ g/mol, $M_w/M_n = 1.22$) were synthesized as previously reported.[33]

PBPEM-*g*-PBA (B1). Samples of 0.115 g of **B0**, 25 mL of deoxygenated *n*-butyl acrylate (BA, 0.174 mol), 0.9 mL of anisole, 2.4 mg of $CuBr_2$ (0.01 mmol), and 172.8 mg of dNbpy (0.43 mmol) were mixed in a Schlenk flask. Then 31 mg of CuBr (0.21 mmol) was added under nitrogen flow. The reaction mixture was heated at 70 °C. The reaction was stopped after 24 h (5.3% BA conversion). The polymer was dried at room temperature, dissolved in 20 mL of chloroform, passed through a neutral alumina column, and dried until constant mass.

PBPEM-*g*-(PBA-*b*-PAN) (B2). A mixture of 0.4 g of **B1**, 23.8 mg of bpy, and 1.0 mg of $CuCl_2$ was dissolved in a mixture of 12 mL of degassed DMF and 6 mL of degassed acrylonitrile. Then 7.5 mg of CuCl was added under nitrogen flow, and the reaction was carried out at 35 °C. The reaction was stopped after 22 h. The polymer was precipitated into 100 mL of methanol, filtered, and dried until constant mass.

PBPEM-*g*-(PBA-*b*-PAN-*b*-PtBA) (B3). A mixture of 150 mg of **B2**, 0.15 mg of $CuCl_2$, and 2.4 μL of PMDETA was dissolved in 6 mL of degassed DMF and 3 mL of deoxygenated *tert*-butyl acrylate. Then 1 mg of CuCl was added under nitrogen. The reaction was carried out at 50 °C. The reaction was stopped after 6 h (12% conversion). The polymer was dried under vacuum, dissolved in DMF, passed through neutral alumina column, precipitated in methanol, and dried until constant weight.

PBPEM-*g*-(PBA-*b*-PAN-*b*-PAA) (B4). Samples of 31.3 mg of **B3**, 0.167 g of TFA, and 12 g of ethylene carbonate were mixed together in a round flask and stirred in an oil bath at 65 °C for 24 h. About 20 g of HPLC-grade water was added to the above mixture, which was then dialyzed against water for 1 day to remove ethylene carbonate. Then, 75 g of water was added to the solution to dilute the system, providing a solution on which the shell cross-linking reaction was performed.

Shell-Cross-Linked PBPEM-*g*-(PBA-*b*-PAN-*b*-PAA) (B5). First, 10.7 mg of 2,2′-(ethylenedioxy)bis(ethylamine) was added to the above **B4** solution and stirred for 2 h followed by the addition of 21.5 mg of carbodiimide (1-[3′-(dimethylamino)propyl]-3-ethylcarbodiimide methiodide). The solution was stirred for 24 h and then dialyzed against water for 4 days, yielding a shell-cross-linked brush solution.

Analysis. Conversion of monomers was measured using a Shimadzu GC14-A gas chromatograph with a FID detector equipped with a J&W Scientific 30 m DB WAX Megabore column. Injector and detector were kept at 250 °C. Molecular weight distribution and evolution of molecular weight over time were measured on a GPC system consisting of a Waters 510 HPLC pump, three Waters UltraStyragel columns (500, 10^3, and 10^5Å), and a Waters 410 DRI detector, with a DMF flow rate of 1.0 mL/min, linear polystyrenes were used as standards. Note that GPC is not a very reliable tool for the determination of molecular weight of molecular brushes, since brushes display a significantly different hydrodynamic behavior than linear polymers. Despite this weakness, GPC can be still used to qualitatively follow progress of the polymerization reaction and provide useful information about the shape of molecular weight distribution curves. Composition of block copolymers has been determined using elemental analysis by Midwest Microlab, LLC.

Tapping Mode Atomic Force Microscopy (TMAFM). TMAFM studies were carried out with the aid of a NanoScope III-M system (Digital Instruments, Santa Barbara, CA), equipped with a J-type vertical engage scanner. Samples were prepared by spin-casting a brush copolymer solution (50−200 μg/mL) in DMF onto freshly cleaved mica substrates. TMAFM observations were performed at room temperature in air using silicon cantilevers with nominal spring constant of 40 N/m and nominal resonance frequency of 300 kHz (standard silicon TESP probes). Typically, the cantilever was oscillated at the frequency at which the oscillation amplitude was equal to 80−95% of amplitude on resonance.

Thermal characterization of bulk samples (6−14 mg) was carried out using Seiko DSC 220 instruments (Seiko Instruments, Inc.) operated at the heating rate 10 °C/min under controlled atmosphere (N_2 flow rate 30−90 mL/min). The Raman spectra were collected on a Jobin Yvon T64000 triple Raman system (ISA, Edison, NJ) in subtractive mode with microprobe sampling optics. The excitation was at 514.5 nm (Ar+ laser, model 95, Lexel Laser, Fremont, CA). Fourier transform infrared spectroscopy (FTIR) was carried out with an FTIR−NIR spectrometer (Mattson ATI Affinity 60AR).

Results and Discussion

1. Synthesis of Molecular Brushes with PAN Block Copolymer Side Chains. The results of synthesis of molecular brushes with homo-, di-, or triblock polymer side chains are listed in Table 1. The preparation of well-defined brushes with homopolymer PBA−Br side chains was carried out using a process similar to that reported earlier.[33] All brushes exhibited narrow molecular weight distribution and good functionality, which is a prerequisite for the block-extension from the side chains. Earlier results revealed that halogen exchange is required for the chain-extension from PBA to PAN.[45,51] Therefore, in order to obtain well-defined block copolymers, CuCl was used instead of CuBr to form the catalyst complex in order to improve the efficiency of the cross-propagation reaction and to slow down the rate of propagation of the PAN block. An example of GPC analysis is displayed in Figure 1 which shows an overlay of progressive traces. All traces were unimodal and symmetrical, and clearly shifted to lower elution volume with increasing time.

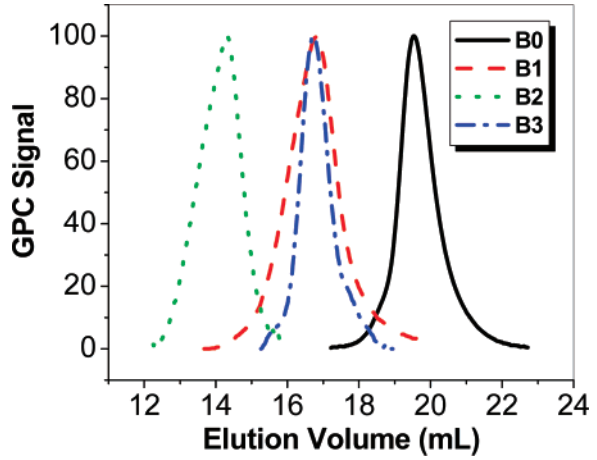

Figure 1. GPC traces of PBPEM (**B0**), PBPEM-*g*-PBA (**B1**), PBPEM-*g*-(PBA-*b*-PAN) (**B2**), and PBPEM-*g*-(PBA-*b*-PAN-*b*-PtBA) (**B3**).

Table 1. Composition of Molecular Brushes

sample	composition	PDI
B0	$(BPEM)_{284}$	1.22
B1	$(BPEM\text{-}g\text{-}(BA)_{21})_{284}$	1.29
B2	$(BPEM\text{-}g\text{-}((BA)_{21}\text{-}b\text{-}(AN)_{60}))_{284}$	1.17
B3	$(BPEM\text{-}g\text{-}((BA)_{21}\text{-}b\text{-}(AN)_{60}\text{-}b\text{-}(tBA)_{55}))_{284}$	1.21
B4	$(BPEM\text{-}g\text{-}((BA)_{21}\text{-}b\text{-}(AN)_{60}\text{-}b\text{-}(AA)_{55}))_{284}$	
B5	shell cross-linked $(BPEM\text{-}g\text{-}((BA)_{21}\text{-}b\text{-}(AN)_{60}\text{-}b\text{-}(AA)_{55}))_{284}$	

Molecular weight distributions were relatively narrow, even at extended polymerization times, as expected for a controlled polymerization.

Further chain-extension of the PBA-*b*-PAN−Cl side chains was then performed with PtBA to generate an outer shell layer for the brushes. Unimodal, symmetrical and progressively shifting GPC traces (Figure 1) were also observed. Interestingly, GPC traces shifted to higher elution volume after *tert*-butyl acrylate polymerization due to changes in the hydrodynamic volume of the polymer in DMF. In all instances, the polydispersity indices were below 1.3. Elemental analysis indicated that mole fraction of the third block increased with the reaction time.

2. Morphology of Molecular Brushes. The high density of side chains present in brush molecules leads to significant congestion along the polymer backbone resulting in an entropically unfavorable extension of the brush backbone, which prevents the polymer from adopting a random coil or globule conformation. The resulting large persistence length of the polymer enables one to use atomic force microscopy to visualize individual brushes with resolution approaching molecular level. In some cases, one can even observe the individual side chains.[3,24,29] Therefore, visualization of brushes by AFM provides direct insights into the overall conformation of individual molecules. Figure 2 presents TMAFM height images of molecular brushes with different polymer side chains. Brushes with homopolymer PBA side chains (**B1**) had the average height $\bar{H} = 1.6$ nm (Figure 2a, Table 2), similar to materials reported in literature.[3] The fine structures of the backbone and side chains of these brushes were clearly resolved (Figure 2a, inset).

The images of brushes with PBA-*b*-PAN side chains (**B2**) were similar to those observed for brushes with PBA side chains (Figure 2b). However, this time the side chain spreading on mica was not clearly evident, perhaps indicating the perturbation induced by the PAN block. Brushes with triblock side chains (**B3**) had dramatically different appearance (Figure 2c), and had the average height $\bar{H} = 5.2$ nm. They were clearly much bulkier and formed characteristic necklace structures. Similar "beading up" has been previously reported for brushes with PBA-*b*-PS side chains,[33] where it has been ascribed to the avoidance of hydrophilic mica surface by hydrophobic PS segments. It appears that similar explanation could be invoked for triblock

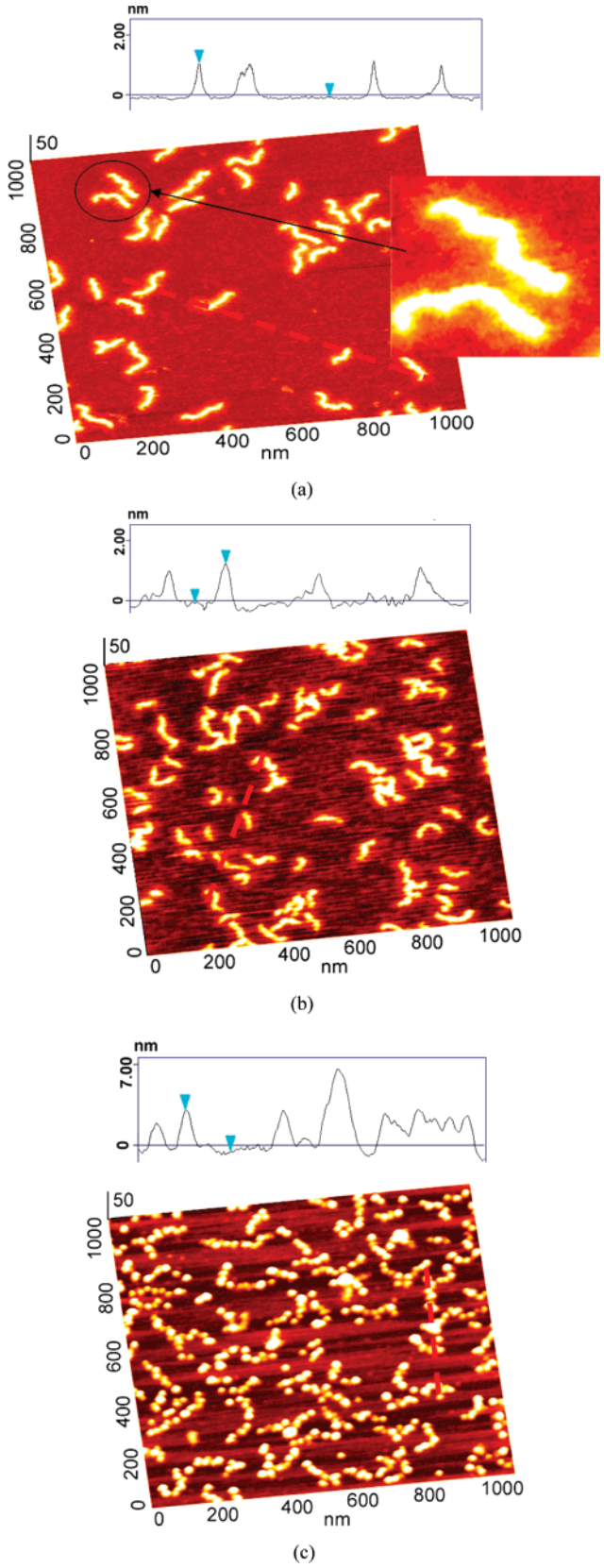

Figure 2. TMAFM height images and cross-section analysis of molecular brushes: (a) PBPEM-*b*-PBA) (**B1**) (inset: magnification of individual brushes); (b) PBPEM-*g*-(PBA-*b*-PAN) (**B2**); (c) PBPEM-*g*-(PBA-*b*-PAN-*b*-PtBA) (**B3**).

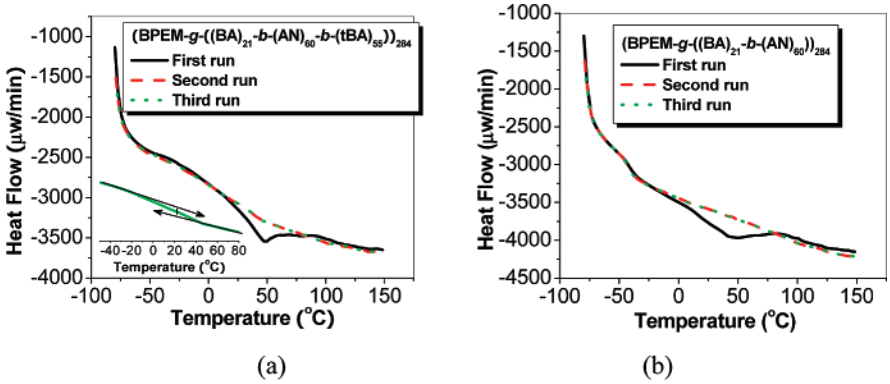

Figure 3. DSC traces of molecular brushes with PAN block copolymer side chains: (a) PBPEM-*g*-(PBA-*b*-PAN-*b*-PtBA) (**B3**); (b) PBPEM-*g*-(PBA-*b*-PAN) (**B2**). Inset: third run of brush **B3**.

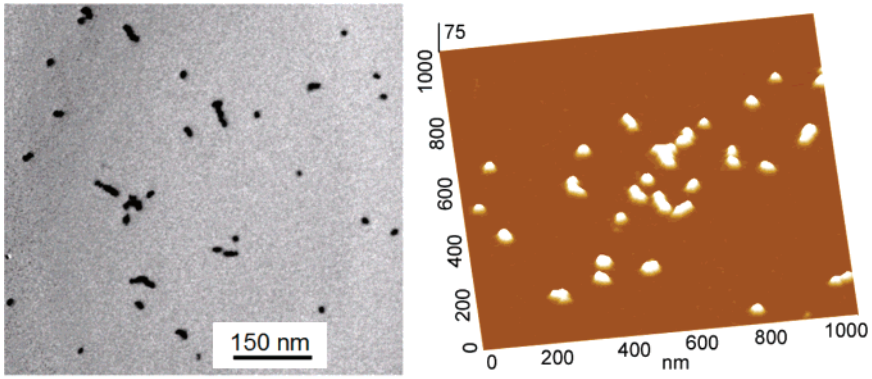

Figure 4. (a) TEM images and (b) TMAFM height images of SC brush precursors.

Table 2. Heights of Different Nanoobjects on the Mica Surface Obtained by AFM

materials	brush[a] **B1**	brush[a] **B2**	brush[b] **B3**	SC brush **B5**	carbon after stabilization	carbon after carbonization
height (nm)	1.6	1.7	5.2	16.5	11.6	5.4

[a] Backbone height. [b] Bead height; SC = shell cross-linked.

brushes with bulky, hydrophobic PtBA segments described here. An additional factor could be partial miscibility of PBA and PtBA, which could be inferred from DSC traces of triblock systems. Those traces revealed only the presence of two glass transition temperatures (T_g): around 23 and around 50 °C (Figure 3a). Whereas the higher T_g could be ascribed to short PAN block, the lower transition was close to the temperature predicted using Fox equation[52] for a homogeneous PBA and PtBA blend. It is important to note that the −50 °C transition due to PBA segments was still observed for diblock PBA-*b*-PAN brushes (Figure 3b).

All the TMAFM observations discussed above were carried out with brushes deposited on mica surfaces. TMAFM images were also obtained for brushes deposited on silicon wafer substrates. Under these circumstances, all the brushes, including brushes with diblock and triblock copolymer side chains, adopted globular conformation or formed aggregates. Such behavior can be the consequence of the lower surface polarity of the native oxide on the silicon surface in comparison with mica. It is known that due to its high polarity and hydrophilicity, under ambient atmosphere mica surface can be covered with a layer of water. There are indications that the presence of this hydration layer is important for facilitating the spreading of PBA chains.[37,38] Silicon surface covered with native oxide is less likely to facilitate such surface spreading.[7]

3. Preparation and Morphology of Shell Cross-Linked Brushes. Low values of heights observed for brushes with PBA, PBA-*b*-PAN, or PBA-*b*-PAN-*g*-PtBA side chains indicate that upon adsorption on the substrate they underwent significant flattening. In order to turn PAN containing brushes into shape-persistent nanoobjects suitable as carbon precursors, they had to be covalently cross-linked, just like shell-cross-linked micelles described earlier.[47] In order to achieve this, brushes with an outer layer of PtBA were hydrolyzed in ethylene carbonate solution in the presence of TFA. The resulting PAA block was cross-linked by a diamine, 2,2′-(ethylenedioxy)-bis(ethylamine), with the aid of a water-soluble carbodiimide, (1-[3′-(dimethyl-amino)propyl]-3-ethylcarbodiimide methiodide). The aqueous solutions were dialyzed against water to remove all byproducts. In order to prevent inter-brush cross-linking, reactions were carried out in dilute solutions. TEM images of shell cross-linked (SC) brushes revealed short rodlike structures (Figure 4a). Shell cross-linked brushes were then spin-coated onto mica and silicon wafers for AFM imaging. AFM images revealed that the morphologies of the stabilized brushes (**B5**) on both substrates were similar and resembled those observed by TEM. The average heights of brush backbones above the substrate were this time much higher than for uncross-linked systems (Table 2), and varied only a little between the samples deposited on mica and silicon wafers (16.5 vs 19.0 nm). Such dramatic

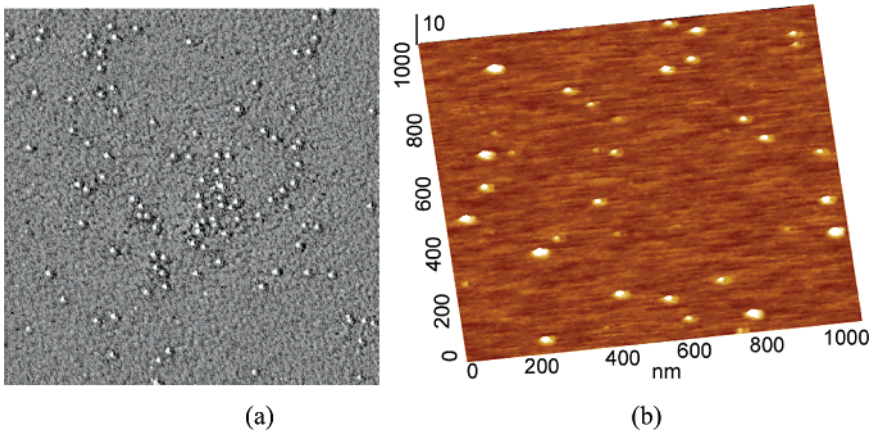

Figure 5. (a) Phase contrast TMAFM image of carbon nanoparticles after 400 °C thermal treatment with molecular brushes with PBA-*b*-PAN side chains (**B2**) (Image size 1.5 × 1.5 μm^2); (b) TMAFM height image of molecular brushes with PBA-*b*-PAN-*b*-PtBA side chains (**B3**) after 250 °C.

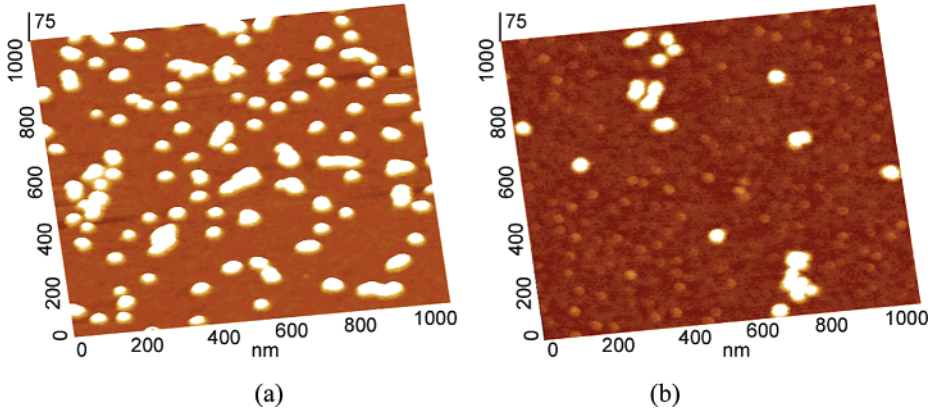

Figure 6. TMAFM height images: (a) carbon nanorods by stabilization of precursors at 250 °C; (b) carbon nanorods by carbonization of precursors at 600 °C following stabilization.

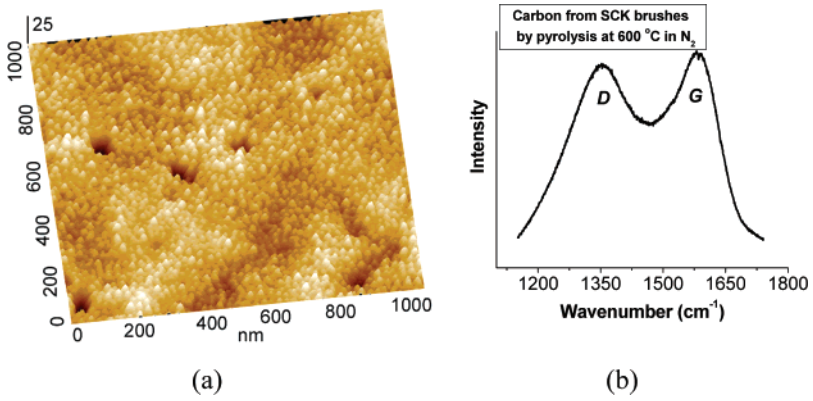

Figure 7. (a) AFM height image and (b) Raman spectrum of multilayer nanostructured carbon from thin film SC brushes pyrolyzed at 600 °C.

increase of height and its insensitivity to the substrate indicated the formation of fixed structures (Figure 4b). It should be noted that in comparison to ABC triblock brushes, shell-cross-linked brushes exhibited a significant decrease of backbone length. It might have been caused by backbone fragmentation due to the strong repulsive force from slightly ionized PAA segments in the course of cross-linking reaction. This phenomenon resembled adsorption-induced fragmentation on mica surface for PBA brushes observed earlier.[41]

4. Conversion of Shell Cross-Linked Brushes into Carbon. Attempts to convert PAN containing brushes into nanostructured carbons pointed out that maintaining the original brush structure upon thermal treatment, without breaking the backbone chains into parts, can be a major challenge. Above 400 °C, all brushes with side chains composed just of PBA-*b*-PAN blocks fragmented into individual nanoparticles, as shown in Figure 5. This suggests that the phase-separated morphology of the brushes inferred from two thermal transitions in DSC traces (Figure 3b) was most likely disrupted upon brush collapse on the surface, preventing effective thermal stabilization. Nevertheless, the residues of brushes were still observed, even after treatment at 600 °C, indicating the formation of small carbon nanoparticles. Brushes with PBA-*b*-PAN-*b*-PtBA side chains exhibited similar behavior following the thermal treatment (Figure 5).

In contrast, the initial shape of shell cross-linked brushes was well maintained after thermal stabilization in an oxidizing

atmosphere. The height of the structures was determined to be 11.6 nm (Figure 6a). After pyrolysis at 600 °C in inert atmosphere, the outer PAA cross-linked layer and inner PBA layer were expected to be degraded with the conversion of PAN into partially graphitic carbon. The AFM images (Figure 6b) showed that the carbon nanostructures, which formed after pyrolysis, indeed preserved the shape of original shell cross-linked brushes, although they underwent significant shrinkage, as reflected by the relatively low height of carbon nanoobjects in comparison with their brush precursors (5.4 vs 19.0 nm).

Thin films of the SC brushes were prepared by drop casting aqueous solutions onto clean silicon wafer substrates. The samples were then subjected to annealing at 250 °C in the presence of air in order to stabilize PAN domains, and subsequently pyrolyzed at 600 °C under N_2 flow. After thermal treatment, SC brush precursors were converted into nanostructured carbon. AFM images of such films (Figure 7a) showed the surface with characteristic round protrusions and rms roughness of 4.0 nm. Such morphology was consistent with the film composed of well-defined, discrete nanoobjects. The carbonized films exhibited characteristics of partially graphitic carbon as evidenced by the presence of broad *D* and *G* bands in the Raman scattering spectra (Figure 7b). FTIR studies showed similar progress of carbonization and CN group evolution as described earlier.[47]

Conclusions

Well-defined molecular brushes containing PAN-based segments in the side chains were prepared by ATRP using a "grafting from" technique. The chosen side chains were PBA-*b*-PAN or PBA-*b*-PAN-*b*-PtBA block copolymers. AFM images if these brushes deposited on flat surfaces revealed flattened wormlike structures. Interestingly, brushes with ABC triblock copolymer side chains (PBA-*b*-PAN-*b*-PtBA) had a necklacelike structure, which may be due to the strong interaction between the terminal PtBA block and the inner PBA block. Shell cross-linked brushes showed increased shape persistence when transferred from solution to substrates, which was demonstrated by the significant increase of their height in comparison to brushes without shell cross-linking. The brush copolymers with PAN segments were then thermally converted into discrete nanostructured carbons. The aspect ratio of resulting carbon nanoobjects was considerably lower than one observed for the brushes from which they were formed. Carbon nanorods with higher aspect ratios could be prepared through the design of brushes with longer backbone, which might require the increase of side chain lengths in order to maintain the persistent shape. The increase of the length of side chains would however carry the risk of causing backbone fragmentation as observed earlier for other system.[41] It is envisioned that carbon nanoobjects such as those described here could find potential use as components of field emitters, lithographic masks, specialized electrodes, etc.

Acknowledgment. The National Science Foundation (T.K., DMR-0304508; K.M., DMR-05 49353) and the CRP Consortium at Carnegie Mellon University are acknowledged for funding.

References and Notes

(1) Beers, K. L.; Gaynor, S. G.; Matyjaszewski, K.; Sheiko, S. S.; Moller, M. *Macromolecules* **1998**, *31*, 9413−9415.
(2) Dziezok, P.; Sheiko, S. S.; Fischer, K.; Schmidt, M.; Moller, M. *Angew. Chem., Int. Ed.* **1997**, *36*, 2812−2815.
(3) Sheiko, S. S.; Moller, M. *Chem. Rev.* **2001**, *101*, 4099−4123.
(4) Sheiko, S. S.; Borisov, O. V.; Prokhorova, S. A.; Moller, M. *Eur. Phys. J. E.* **2004**, *13*, 125−131.
(5) Sheiko, S. S.; da Silva, M.; Shirvaniants, D.; LaRue, I.; Prokhorova, S.; Moeller, M.; Beers, K.; Matyjaszewski, K. *J. Am. Chem. Soc.* **2003**, *125*, 6725−6728.
(6) Zhang, M. F.; Drechsler, M.; Muller, A. H. E. *Chem. Mater.* **2004**, *16*, 537−543.
(7) Cheng, G. L.; Boker, A. A.; Zhang, M. F.; Krausch, G.; Muller, A. H. E. *Macromolecules* **2001**, *34*, 6883−6888.
(8) Zhang, B.; Zhang, S. J.; Okrasa, L.; Pakula, T.; Stephan, T.; Schmidt, M. *Polymer* **2004**, *45*, 4009−4015.
(9) Djalali, R.; Li, S. Y.; Schmidt, M. *Macromolecules* **2002**, *35*, 4282−4288.
(10) Saariaho, M.; Subbotin, A.; Szleifer, I.; Ikkala, O.; ten Brinke, G. *Macromolecules* **1999**, *32*, 4439−4443.
(11) Sumerlin, B.; Matyjaszewski, K. In *Macromolecular Engineering: From Precise Macromolecular Synthesis to Macroscopic Materials Properties and Applications*; Matyjaszewski, K., Gnanou, Y., Leibler, L., Eds.; Wiley-VCH: Weinheim, Germany, 2007; Vol. 2, pp 1103−1135.
(12) Zhang, M.; Mueller, A. H. E. *J. Polym. Sci., Polym. Chem.* **2005**, *43*, 3461−3481.
(13) Pakula, T.; Zhang, Y.; Matyjaszewski, K.; Lee, H.-i.; Boerner, H.; Qin, S.; Berry, G. C. *Polymer* **2006**, *47*, 7198−7206.
(14) Schappacher, M.; Deffieux, A. *Macromolecules* **2000**, *33*, 7371−7377.
(15) Tsukahara, Y.; Tsutsumi, K.; Yamashita, Y.; Shimada, S. *Macromolecules* **1990**, *23*, 5201−5208.
(16) Wang, J. S.; Matyjaszewski, K. *J. Am. Chem. Soc.* **1995**, *117*, 5614−5615.
(17) Matyjaszewski, K.; Xia, J. H. *Chem. Rev.* **2001**, *101*, 2921−2990.
(18) Matyjaszewski, K.; Davis, T. P. Eds. *Handbook of radical polymerization*; John Wiley & Sons: Hoboken, NJ, 2002.
(19) Braunecker, W. A.; Matyjaszewski, K. *Prog. Polym. Sci.* **2007**, *32*, 93−146.
(20) Yagci, Y.; Tasdelen, M. A. *Prog. Polym. Sci.* **2006**, *31*, 1133−1170.
(21) Hadjichristidis, N.; Iatrou, H.; Pitsikalis, M.; Mays, J. *Prog. Polym. Sci.* **2006**, *31*, 1068−1132.
(22) Borner, H. G.; Duran, D.; Matyjaszewski, K.; da Silva, M.; Sheiko, S. S. *Macromolecules* **2002**, *35*, 3387−3394.
(23) Matyjaszewski, K.; Qin, S. H.; Boyce, J. R.; Shirvanyants, D.; Sheiko, S. S. *Macromolecules* **2003**, *36*, 1843−1849.
(24) Neugebauer, D.; Zhang, Y.; Pakula, T.; Sheiko, S. S.; Matyjaszewski, K. *Macromolecules* **2003**, *36*, 6746−6755.
(25) Qin, S. H.; Matyjaszewski, K.; Xu, H.; Sheiko, S. S. *Macromolecules* **2003**, *36*, 605−612.
(26) Sheiko, S. S.; Prokhorova, S. A.; Beers, K. L.; Matyjaszewski, K.; Potemkin, I. I.; Khokhlov, A. R.; Moller, M. *Macromolecules* **2001**, *34*, 8354−8360.
(27) Pietrasik, J.; Sumerlin, B. S.; Lee, H.-i.; Gil, R. R.; Matyjaszewski, K. *Polymer* **2007**, *48*, 496−501.
(28) Sumerlin, B. S.; Neugebauer, D.; Matyjaszewski, K. *Macromolecules* **2005**, *38*, 702−708.
(29) Li, C. M.; Gunari, N.; Fischer, K.; Janshoff, A.; Schmidt, M. *Angew. Chem., Int. Ed.* **2004**, *43*, 1101−1104.
(30) Lee, H.-i.; Matyjaszewski, K. *Polym. Prepr.* **2005**, *46*, 144−145.
(31) Pietrasik, J.; Sumerlin, B. S.; Lee, R. Y.; Matyjaszewski, K. *Macromol. Chem. Phys.* **2007**, *208*, 30−36.
(32) Lee, H.-i.; Pietrasik, J.; Matyjaszewski, K. *Macromolecules* **2006**, *39*, 3914−3920.
(33) Borner, H. G.; Beers, K.; Matyjaszewski, K.; Sheiko, S. S.; Moller, M. *Macromolecules* **2001**, *34*, 4375−4383.
(34) Lee, H.; Jakubowski, W.; Matyjaszewski, K.; Yu, S.; Sheiko, S. S. *Macromolecules* **2006**, *39*, 4983−4989.
(35) Ishizu, K.; Kakinuma, H. *J. Polym. Sci., Polym. Chem.* **2005**, *43*, 63−70.
(36) Lecommandoux, S.; Chécot, F.; Borsali, R.; Schappacher, M.; Deffieux, A.; Brulet, A.; Cotton, J. P. *Macromolecules* **2002**, *35*, 8878−8881.
(37) Gallyamov, M. O.; Tartsch, B.; Khoklov, A. R.; Sheiko, S. S.; Borner, H. G.; Matyjaszewski, K.; Moller, M. *Macromol. Rapid Commun.* **2004**, *25*, 1703−1707.
(38) Gallyamov, M. O.; Tartsch, B.; Khokhlov, A. R.; Sheiko, S. S.; Borner, H. G.; Matyjaszewski, K.; Moller, M. *Chem.—Eur. J.* **2004**, *10*, 4599−4605.
(39) Rathgeber, S.; Pakula, T.; Wilk, A.; Matyjaszewski, K.; Beers Kathryn, L. *J. Chem. Phys.* **2005**, *122*, 124904−13.
(40) Rathgeber, S.; Pakula, T.; Wilk, A.; Matyjaszewski, K.; Lee, H.-i.; Beers, K. L. *Polymer* **2006**, *47*, 7318−7327.
(41) Sheiko, S. S.; Sun, F. C.; Randall, A.; Shirvanyants, D.; Rubinstein, M.; Lee, H.; Matyjaszewski, K. *Nature (London)* **2006**, *440*, 191−194.
(42) Bates, F. S.; Fredrickson, G. H. *Phys. Today* **1999**, *52*, 32−38.
(43) Sun, F.; Sheiko, S. S.; Moller, M.; Beers, K.; Matyjaszewski, K. *J. Phys. Chem. A* **2004**, *108*, 9682−9686.

(44) Cheng, C.; Qi, K.; Khoshdel, E.; Wooley, K. *J. Am. Chem. Soc.* **2006**, *128*, 6808−6809.
(45) Kowalewski, T.; Tsarevsky, N. V.; Matyjaszewski, K. *J. Am. Chem. Soc.* **2002**, *124*, 10632−10633.
(46) Kowalewski, T.; McCullough, R. D.; Matyjaszewski, K. *Eur. Phys. J. E.* **2003**, *10*, 5−16.
(47) Tang, C.; Qi, K.; Wooley, K.; Matyjaszewski, K.; Kowalewski, T. *Angew. Chem., Int. Ed.* **2004**, *43*, 2783−2787.
(48) Tang, C.; Tracz, A.; Kruk, M.; Zhang, R.; Smilgies, D. M.; Matyjaszewski, K.; Kowalewski, T. *J. Am. Chem. Soc.* **2005**, *127*, 6918−6919.
(49) (a) Keller, R. N.; Wycoff, H. D. *Inorg. Synth.* **1946**, *2*, 1−4. (b) Xia, J.; Matyjaszewski, K. *Macromolecules* **1999**, *32*, 2434−2437.
(50) Matyjaszewski, K.; Patten, T. E.; Xia, J. H. *J. Am. Chem. Soc.* **1997**, *119*, 674−680.
(51) (a) Tang, C.; Kowalewski, T.; Matyjaszewski, K. *Macromolecules* **2003**, *36*, 1465−1473. (b) Matyjaszewski, K.; Shipp, D. A.; McMurtry, G. P.; Gaynor, S. G.; Pakula, T. *J. Polym. Sci., Part A: Polym. Chem.* **2000**, *38*, 2023−2031. (c) Davis, K. A.; Matyjaszewski, K. *Adv. Polym. Sci.* **2002**, *159*, 1−166.
(52) Fox, T. G. *Bull. Am. Phys. Soc.* **1956**, *1*, 123−125.

MA070892O